

Spin-gapped magnets with weak anisotropies II: Effects of exchange and Dzyaloshinsky-Moriya anisotropies on thermodynamic characteristics

Abdulla Rakhimov¹, Asliddin Khudoyberdiev², B. Tanatar¹

¹*Department of Physics, Bilkent University, Bilkent, 06800 Ankara, Turkey*

²*Institute of Nuclear Physics, Tashkent 100214, Uzbekistan*

(Dated: November 5, 2021)

Abstract

We study the modification of low temperature properties of quantum magnets such as magnetization, heat capacity, energy spectrum, and densities of condensed and noncondensed quasiparticles (triplons) due to anisotropies in the framework of mean-field based approach. We show that in contrast to exchange anisotropy (EA) interaction, Dzyaloshinsky-Moriya (DM) interaction modifies the physics dramatically. Particularly, it changes the sign of the anomalous density in the whole range of temperatures. Its critical behavior is slightly modified also by the EA. We have found that the shift of the critical temperature of phase transition (or crossover caused by DM interaction) is positive and significant. Using the experimental data on the magnetization of the compound TlCuCl_3 , we have found optimal values for the strengths of EA and DM interactions. The spectrum of the energy of low lying excitations has also been investigated and found to develop a linear dispersion similar to Goldstone mode with a negligibly small anisotropy gap.

I. INTRODUCTION

Presently, it is well established that there is a class of quantum magnets whose low temperature properties could be described within the paradigm of Bose-Einstein condensation (BEC) of quasiparticles referred as triplons[1]. Experimentally this is confirmed by studying the critical exponents as well as the magnetic excitation spectrum of such compounds at low temperatures. A good example is the critical exponent ϕ , associated with phase boundary $H_c(T)$, that divides the paramagnetic and field induced canted XY antiferromagnetic phase of several quantum magnets, $H_c(T) - H_c(0) \propto T^\phi$. This exponent approaches its expected value of $3/2$, which is typical for a system with BEC, when the window of low temperatures is rather reduced[2]. Recent experimental investigations were conducted by Zhou *et al.*[3] for the entire magnetization process of TlCuCl_3 up to the magnetic field of 100 T at temperature 2 K. They also analyzed magnetic field-temperature phase boundary dependence around the critical fields H_{c1} and H_{c2} and concluded that for both critical phase boundaries the critical exponents are $\phi \approx 3/2$. Another experimental evidence is offered by the properties of the excitation spectrum in the BEC state which has been theoretically predicted to be a gapless Goldstone mode associated with the spontaneous breaking of rotational symmetry by the staggered order. Thus, the presence of a spin-wave like mode with a linear mode dispersion, $E_k \sim ck$, is a convincing signal for the existence of BEC in this class of quantum magnets[4]. Therefore, one may conclude that at low temperatures thermodynamic properties of such materials are determined mainly (but not only) by the condensation of triplons[5].

Theoretically, the system of triplons can be described by the following effective Hamiltonian:

$$H_{iso} = \int d^3r \left[\psi^\dagger(\vec{r})(\hat{K} - \mu)\psi(\vec{r}) + \frac{U}{2}(\psi^\dagger(\vec{r})\psi(\vec{r}))^2 \right], \quad (1.1)$$

where $\psi(r)$ is the bosonic field operator, \hat{K} is the kinetic energy operator which defines the bare triplon dispersion ε_k in momentum space and U is the strength of contact interaction describing a strong short-range triplon-triplon repulsion. The Hamiltonian in Eq. (1.1) is formally the same as used for BEC of atomic gases[6]. However, there is a small difference in the strategy. In tasks related to atomic Bose gases the number of particles N is assumed to be fixed, while the chemical potential $\mu(N, T)$ is to be calculated say, by the relation

$N \sim \sum_k 1/[e^{\beta(\varepsilon_k - \mu)} - 1]$, where β is the inverse temperature. As to the triplon gas, the chemical potential in Eq. (1.1) characterizes an additional direct contribution to the triplon energy due to the external magnetic field H , giving $\mu = g\mu_B(H - H_c)$ where g is the electron Landé factor, $\mu_B = 0.672 \text{ KT}^{-1}$ is the Bohr magneton and H_c is the critical magnetic field which defines the gap $\Delta_{ST} = g\mu_B H_c$ between singlet and triplet states. In the field induced BEC, μ is assumed to be an input parameter, from which the total number of triplons can be calculated. Moreover, for homogenous atomic gases one may use simple quadratic bare dispersion $\varepsilon_k = k^2/2m$ with a good accuracy, while for spin-gapped quantum magnets a more complicated form of bare dispersion is needed.[2, 7–10]

It is well known that the Hamiltonian in Eq. (1.1) leads to a gapless Bogoliubov dispersion, $E_k = \sqrt{\varepsilon_k} \sqrt{\varepsilon_k + 2U\rho} \approx ck + \mathcal{O}(k^3)$ at low temperatures, with density $\rho = N/V$ and sound velocity c . However, low frequency electron spin resonance (ESR) measurements on some materials, such as TlCuCl_3 [11, 12], $(\text{C}_4\text{H}_{12}\text{N}_2)(\text{Cu}_2\text{Cl}_6)$ [13], Cs_2CuCl_4 [14], DTN [15] gave evidence for a tiny spin gap. The origin of this gap is due to exchange anisotropy (EA) or Dzyaloshinsky-Moriya (DM) interactions, which should be taken into account in the theoretical description, and particularly, in the effective model Hamiltonian[16]. A simpler extended Hamiltonian such as Eq. (1.1) including EA and DM interactions was proposed by Sirker *et al.*[17]

$$H_{\text{aniz}} = \int d^3r \{ \psi^+(\vec{r})(\hat{K} - \mu)\psi(\vec{r}) + \frac{U}{2}(\psi^+(\vec{r})\psi(\vec{r}))^2 + \frac{\gamma}{2}[\psi^+(\vec{r})\psi^+(\vec{r}) + \psi(\vec{r})\psi(\vec{r})] + i\gamma'[\psi(\vec{r}) - \psi^+(\vec{r})] \} \quad (1.2)$$

where γ and γ' are interaction strengths of EA and DM interactions, respectively ($\gamma \geq 0$, $\gamma' \geq 0$). Thus, once the Hamiltonian is given, one first separates fluctuations as $\psi = \xi\sqrt{\rho_0} + \tilde{\psi}$, where $\xi = e^{i\Theta}$ and ρ_0 are the phase of the condensate wave function and its magnitude, respectively; and then introducing second quantization, $\tilde{\psi}(\vec{r}) = \sum_k e^{i\vec{k}\vec{r}} a_k$, $\tilde{\psi}^+(\vec{r}) = \sum_k e^{-i\vec{k}\vec{r}} a_k^+$, makes an attempt to diagonalize the Hamiltonian H with respect to creation (a^+) and annihilation (a) operators. As a result, analytical expressions for quasi-particle (bogolon) dispersion E_k and some other quantities may be obtained. In the present work we shall take into account anomalous averages $\sigma = \sum_k \sigma_k = \frac{1}{2} \sum_k (\langle a_k a_{-k} \rangle + \langle a_k^\dagger a_{-k}^\dagger \rangle)$ (σ -anomalous density) based on Hartree-Fock-Bogoliubov approach, which was neglected in Ref. [17]. This allows one to obtain continuous magnetization across the BEC transition, which would be discontinuous otherwise, in the so-called Hartree-Fock-Popov (HFP)

approximation with $\sigma = 0$ [18].

In order to get more information about thermodynamics of the system we exploit the grand canonical thermodynamic potential Ω , which may be evaluated in the path integral formalism[6, 19–21]. This will be convenient to study the modification of the condensate wave function, entropy $S = -(\partial\Omega/\partial T)$, heat capacity $C_H = T(\partial S/\partial T)$, magnetization $M = -(\partial\Omega/\partial H)$, and possibly other physical quantities due to anisotropies.

In our previous work[22] we have derived an explicit expression for Ω of a homogenous system of bosons, described by the Hamiltonian in Eq. (1.2). Minimization of thermodynamic potential with respect to the phase ξ and condensate fraction ρ_0 , together with the requirement of dynamical stability of BEC led to following conclusions (see Table 1 of Ref. [22]).

(a) The condensate has a definite phase[23], which is independent of temperature or magnetic field.

(b) The phase angle Θ may have only discrete values, namely $\Theta = \pi n$ and $\Theta = \pi/2 + 2\pi n$ ($n = 0, \pm 1, \pm 2, \dots$) for an equilibrium system of bosons without and with DM interaction, respectively.

(c) The presence of a weak DM interaction even with a tiny strength smears out the phase transition from BEC to normal phase into a crossover, i.e, the condensate fraction may vanish only asymptotically by increasing the temperature. Besides, the DM interaction fixes the direction of staggered magnetization, predicted by Matsumoto *et al.*[24], based on symmetry considerations.

In the present work we shall study the modification of some physical observables due to EA and DM anisotropies given by Eq. (1.2).

The rest of this paper is organized as follows. In Section II we discuss the properties of main equations of the present approach. In Section III we analyze the role of anisotropies for the thermodynamic parameters such as anomalous density, self-energies, magnetization and heat capacity. We compare our theoretical results with experimental ones for the TlCuCl_3 compound in Section IV and summarize our main results in Section V.

Throughout the paper we adopt the units $k_B \equiv 1$ for the Boltzmann constant, $\hbar \equiv 1$ for the Planck constant, and $V \equiv 1$ for the unit cell volume. In these units the energies are measured in Kelvin (K), the mass m is expressed in K^{-1} , the magnetic susceptibility χ for the magnetic fields measured in Tesla (T) has the units of K/T^2 , while the momentum and

specific heat C_H are dimensionless. Particularly, the Bohr magneton is $\mu_B = \hbar e/2m_0c = 0.671668 \text{ K/T}$, where m_0 is the free electron mass, and e is the fundamental charge.

II. PROPERTIES OF MAIN EQUATIONS FOR SELF ENERGIES

One of the main quantities to describe the low temperature properties of ultracold bosonic systems is the dispersion relation for quasiparticles, which is supposed to be written as $E_k = \sqrt{\varepsilon_k + X_1}\sqrt{\varepsilon_k + X_2}$, in general. Here ε_k is the bare dispersion of triplons[25] and the quantities $X_{1,2}$ are related to the ordinary normal Σ_n , and anomalous Σ_{an} , self-energies as follows $X_{1,2} = \Sigma_n \pm \Sigma_{an} - \mu$. The self-energies $X_{1,2}$ and the condensate fraction are the solutions to the following equations[22]:

$$X_1 = 2U\rho + U\sigma - \mu + \frac{U\rho_0(\xi^2 + \bar{\xi}^2)}{2} + \gamma + \frac{2\gamma'^2 D_1}{X_2^2} \quad (2.3a)$$

$$X_2 = 2U\rho - U\sigma - \mu - \frac{U\rho_0(\xi^2 + \bar{\xi}^2)}{2} - \gamma - \frac{2\gamma'^2 D_2}{X_2^2} \quad (2.3b)$$

$$\frac{\partial\Omega}{\partial\rho_0} = \cos 2\Theta(U\sigma + \gamma) + U(\rho_0 + 2\rho_1) - \mu - \frac{\gamma' \sin \Theta}{\sqrt{\rho_0}} = 0 \quad (2.3c)$$

where

$$A'_1 = \frac{\partial A}{\partial X_1} = \frac{1}{8} \sum_k \frac{(E_k W'_k + 4W_k)}{E_k} \quad (2.4a)$$

$$A'_2 = \frac{\partial A}{\partial X_2} = \frac{1}{8} \sum_k \frac{(\varepsilon_k + X_1)^2 (E_k W'_k - 4W_k)}{E_k^3} \quad (2.4b)$$

$$B'_1 = \frac{\partial B}{\partial X_1} = \frac{1}{8} \sum_k \frac{(\varepsilon_k + X_2)^2 (E_k W'_k - 4W_k)}{E_k^3} \quad (2.4c)$$

$$D_1 = \frac{A'_1}{\bar{D}}; \quad D_2 = \frac{B'_1}{\bar{D}}; \quad \bar{D} = A_1'^2 - A_2' B_1' \quad (2.4d)$$

$$W_k = \frac{\coth(\beta E_k/2)}{2}; \quad W'_k = \beta(1 - 4W_k^2) = \frac{-\beta}{\sinh^2(\beta E_k/2)}. \quad (2.4e)$$

In the above equations $A = \rho_1 - \sigma$, $B = \rho_1 + \sigma$ and the normal ρ_1 and anomalous σ densities are given below. In the Hartree-Fock-Bogoliubov approximation these self-energies play an essential role. Thus, we first study their properties and then evaluate physical observables under consideration. For simplicity, we rewrite Eqs. (2.3) and (2.4) separately for the cases with ($\gamma' = 0$) and without ($\gamma' \neq 0$) DM interactions, taking into account that for these cases $\xi = \pm 1$ and $\xi = i$, respectively.

A. mode 1: $\gamma' = 0, \gamma \neq 0, \xi = 1$

This mode corresponds to the case when only EA is present. Here we have both phases, BEC and normal, which are sharply separated by the critical temperature T_c defined by the equation $\rho_0(T = T_c) = 0$. The condensate fraction is given in BEC phase by $\rho_0 = (\Delta - 2\gamma - U\sigma)/U$, where Δ is the solution of the algebraic equation

$$\Delta = \mu + 2U(\sigma - \rho_1) + 5\gamma = U(\rho_0 + \sigma) + 2\gamma \quad (2.5)$$

where the normal ρ_1 and anomalous σ densities are given by following general expressions

$$\rho_1 = \sum_k \left[\frac{W_k(\varepsilon_k + X_1/2 + X_2/2)}{E_k} - \frac{1}{2} \right] \equiv \sum_k \rho_{1k} \quad (2.6a)$$

$$\sigma = \frac{(X_2 - X_1)}{2} \sum_k \frac{W_k}{E_k} \equiv \sum_k \sigma_k \quad (2.6b)$$

with $X_1 = 2\Delta$, $X_2 = 2\gamma$, $E_k = \sqrt{(\varepsilon_k + 2\Delta)(\varepsilon_k + 2\gamma)}$, $\rho = \rho_0 + \rho_1$.

In the normal phase $\rho_0(T > T_c) = 0$, the self-energies X_1 , X_2 in the dispersion relation $E_k \equiv \omega_k = \sqrt{(\varepsilon_k + X_1)(\varepsilon_k + X_2)}$ are given as

$$X_{1,2}(T > T_c) = 2U\rho - \mu \pm (U\sigma + \gamma) \quad (2.7)$$

where the total triplon density is

$$\rho(T > T_c) = \sum_k \frac{1}{e^{\beta\omega_k} - 1}. \quad (2.8)$$

Explicit expressions for other quantities are moved to the Appendix for convenience.

Note that our mean-field based main equations are rather general leading to well known approximations used in the literature for the isotropic case, when all anisotropies are neglected. Particularly, one may derive Hartree-Fock-Popov approximation and simple Bogoliubov approximations as follows.

- **HFP approximation** This is widely used in literature and obtained simply by neglecting σ and γ in Eq.(2.5) resulting in the following equation for the condensate fraction

$$\rho_0 = \rho - \rho_1 = \rho - \sum_k \left[\frac{W_k(\varepsilon_k + U\rho_0)}{\sqrt{\varepsilon_k}\sqrt{\varepsilon_k + 2U\rho_0}} - \frac{1}{2} \right]. \quad (2.9)$$

- **Bogoliubov approximation.** Further, at zero temperature, making formal replacement $\rho_0 \rightarrow \rho$ on the right hand side of Eq. (2.9) gives

$$\frac{\rho_0}{\rho} = 1 - \frac{1}{2\rho} \sum_k \left[\frac{\varepsilon_k + U\rho}{\sqrt{\varepsilon_k} \sqrt{\varepsilon_k + 2U\rho}} - 1 \right]. \quad (2.10)$$

For infinite uniform system with $\varepsilon = \vec{k}^2/2m$, $|k| = 0, \dots, \infty$, one may evaluate the momentum integration in Eq. (2.10) to obtain the following well known formula[18, 21]

$$\frac{\rho_0}{\rho} = 1 - \frac{8\sqrt{\rho a_s^3}}{3\sqrt{\pi}} \quad (2.11)$$

where $a_s = Um/4\pi$ is the s-wave scattering length. Remarkably, the quantum depletion given by the second term on the right hand side of Eq. (2.11), as well as the energy dispersion in Eq. (2.10) $E_k = \sqrt{\varepsilon_k} \sqrt{\varepsilon_k + 2U\rho}$ were proposed by Bogoliubov more than seventy years ago[26] and has been one of the cornerstones of our understanding of interacting quantum fluids[27].

B. mode 2: $\gamma' \neq 0, \gamma \neq 0, \xi = i$

Here both EA and DM interactions are present. The main equations for self-energies X_1 and X_2 are obtained from Eq. (20) of Ref. [22] by setting $\xi = i$,

$$X_1 = 2U\sigma + 2\gamma + \frac{\gamma'}{\sqrt{\rho_0}} + \frac{2\gamma'^2 D_1}{X_2^2}, \quad (2.12a)$$

$$X_2 = 2U\rho_0 + \frac{\gamma'}{\sqrt{\rho_0}} - \frac{2\gamma'^2 D_2}{X_2^2}. \quad (2.12b)$$

The equation for the condensate fraction ρ_0 may be presented in the following dimensionless compact form

$$r_0^3 + Pr_0 + Q = 0 \quad (2.13)$$

where we have introduced $P = -\bar{\sigma} + 2(\bar{\rho}_1 - 1 - \bar{\gamma})$, $Q = -2\bar{\gamma}'/\sqrt{\rho_{c0}}$, $r_0^2 = \rho_0/\rho_{c0}$, $\bar{\sigma} = \sigma/\rho_{c0}$, $\bar{\rho}_1 = \rho_1/\rho_{c0}$, $\bar{\gamma} = \gamma/\mu$, $\bar{\gamma}' = \gamma'/\mu$ in which ρ_{c0} is the critical density of pure BEC, $\rho_{c0} = \mu/2U$.

In general, one has to solve these three coupled nonlinear algebraic equations for the unknown quantities X_1 , X_2 and r_0 at a given temperature and magnetic field. Clearly, in such cases it is important to guess the initial values of $X_1(T)$ and $X_2(T)$, since the solutions

are not unique. For this purpose it will be convenient to start from a higher temperature, say $T \approx 15$ K, where $\sigma(T \gg T_c) \approx 0$, $\gamma'^2/X_2^2 \rightarrow 0$ and hence Eqs. (2.12) are simplified to

$$Z_1 = \frac{\gamma}{\mu} - \frac{Q}{4r_0}, \quad Z_2 = \frac{r_0^2}{2} - \frac{Q}{4r_0}, \quad (2.14)$$

where $Z_1 = X_1/2\mu$ and $Z_2 = X_2/2\mu$.

1. High temperatures

For a weak EA interaction, $\gamma/\mu \ll 1$ Eqs. (2.14) coincide with those obtained by Sirker *et al.*[28] within the HFP approximation with $\sigma = \gamma = 0$, and may be solved easily by inserting Z_1, Z_2 into Eq. (2.13), thus by reducing the system of three coupled equations into one cubic algebraic equation with respect to r_0 . It is clear that in this regime Eqs. (2.3a) and (2.3b) are simplified as

$$X_1(T \gg T_c) \approx X_2(T \gg T_c) = 2U\rho - \mu \quad (2.15)$$

where $\rho = \rho_0 + \rho_1$ is the total density of triplons, and T_c is defined as $(d\rho/dT)|_{T=T_c} = 0$, $(d^2\rho/dT^2)|_{T=T_c} \geq 0$ and hence the normal Σ_n and anomalous Σ_{an} self-energies have the form

$$\Sigma_n = \mu + \frac{X_1 + X_2}{2} \approx 2U\rho, \quad \Sigma_{an} = \frac{X_1 - X_2}{2} \approx 0. \quad (2.16)$$

In Fig. 1, we present typical solutions of Eqs. (2.12) and (2.13) as a function of temperature for $\gamma' = 0.1$ K and $\gamma = 0$. It is seen that at high temperatures X_1 and X_2 overlap with that of pure BEC with $\gamma = \gamma' = 0$ in accordance with Eq. (2.15). Therefore, the effect of anisotropy on self-energies is negligibly small at high temperatures. On the other hand, the effect of DM interaction on the condensate fraction is rather significant, as it is seen from Fig. 1(c).

In fact, since in the presence of DM interaction the parameter Q is finite, Eq. (2.13) does not have a zero solution, as illustrated in Fig. 1(c). Strictly speaking, at any temperature there exists a finite condensate fraction. Thus, comparing $\rho_0(T)$ for pure BEC (dotted curve) with that for the case of DM interaction (solid curve) in Fig. 1(c) one may conclude that, DM anisotropy smears out BEC transition into a crossover.

2. Low temperatures

Moreover, comparing those curves in Fig. 1(c) at low temperatures one may note that the DM interaction enhances the condensate fraction significantly. For example, the condensate fraction at $T = 0$ for $\gamma' = 0.1$ K is nearly 2.7 times larger than that for $\gamma' = 0$, corresponding to the isotropic case.

We now discuss the low temperature behavior of self-energies X_1 and X_2 . As it is seen from Fig. 1 in this region in the approach by Sirker et al.[28] X_1 and X_2 are nearly of the same order, while in the present approximation X_1 is much smaller than X_2 , ($X_1/X_2 \approx 10^{-4}$). The main reason of this difference is that in the present approximation the anomalous density has not been neglected, and besides, the DM interaction is taken into account up to the second order in the strength. Now coming back to the main equations for X_1 and X_2 one may note that, at low temperatures, D_1 in Eqs. (2.12a) given by Eqs. (2.4) becomes negligibly small, while D_2 in Eq. (2.12b) remains finite. Thus, Eq. (2.12a) with $\gamma = 0$ and the difference $X_2 - X_1$ can be written as

$$X_1(T \rightarrow 0) \approx 2U\sigma + \frac{\gamma'}{\sqrt{\rho_0}} \quad (2.17a)$$

$$(X_2 - X_1)|_{T \rightarrow 0} \approx 2U(\rho_0 - \sigma) - \frac{2\gamma'^2 D_2}{X_2^2}. \quad (2.17b)$$

From Eq.(2.17a) it can be immediately seen that, since $\sigma > 0$,¹ $X_1(T \rightarrow 0) \neq 0$ when $\gamma' \neq 0$, that is the gap in the quasiparticle dispersion $E_k = \sqrt{(\varepsilon_k + X_1)(\varepsilon_k + X_2)}$ can never be closed for $\gamma' \neq 0$ (we shall come back to this point in Section IV). As to the difference $X_2 - X_1$, it becomes large i.e., $X_2 \gg X_1$ due to the presence of the last term in Eq. (2.17b) with $D_2 > 0$, since lowering the temperature leads also to a decrease in X_2 .

C. Upper boundary for strength of DM interaction

In our previous work[22], requiring positiveness of self-energies, X_1 and X_2 , we have found a boundary condition for the strength of EA interaction as $\gamma \leq U|\sigma|$. Now we address the question whether a similar condition be found for the strength of DM interaction γ' .

First, we note that Eq. (2.13) for r_0 has a positive solution regardless the sign (and value)

¹ See the next section.

of the parameter P . In fact, since $\gamma' > 0$, the number of sign changes in this equation is equal to unity, it has exactly one positive solution due to Descartes' Rule of Signs. Hence, in the approximation suggested by Ref. [17], the right hand side of Eqs. (2.14) are positive for any $\gamma' > 0$. Thus, when we neglect σ and use the approximation linear in γ' , there is no upper bound for the strength of DM interaction, γ' . However, when we go beyond such an approximation, we have to deal with Eqs. (2.3a) and (2.3b), where the last terms with γ'^2 play an important role for large γ' . By examining the coefficients of γ'^2 , namely D_1 and D_2 given in Eqs. (2.4) one may find that $D_2 > 0$ and $D_1 < 0$ at any temperature. Now, it can be understood that at large values of γ' , the last term in Eq. (2.12b) will dominate over the first and second terms, making the right hand side of this equation negative. Actual numerical analysis for TlCuCl_3 show that this happens at $\gamma' > 0.7\text{K}$ for $H \leq 20\text{ T}$. In reality, γ' is rather small: $\gamma'_{\text{optimum}} \approx 0.02\text{ K}$ (see Section IV). Anyway, in contrast to approximation used in Ref. [17], the present approach, taking into account γ' up to the second order, is able to predict an upper bound for the strength of DM interaction $\gamma'_{\text{max}} \approx 0.7\text{K}$, beyond which this interaction destroys the condensate of triplons.

III. SENSITIVITY OF THERMODYNAMIC CHARACTERISTICS TO ANISOTROPIES

In Ref. [22] we have shown that the presence of H_{EA} and D_{DM} terms in the bosonic Hamiltonian with contact interaction may significantly modify the phase and the condensate fraction of BEC. Now we discuss their influence on some physical quantities .

A. Anomalous density and self-energy

Firstly we show that even a tiny DM interaction changes the sign of anomalous density σ , which is negative for pure BEC in finite systems. In fact, subtracting Eq. (2.12b) from Eq. (2.12a) and using Eq. (2.6b) with $\gamma = 0$, one obtains

$$\sigma = \tilde{S}(\rho_0 - \sigma) - \frac{\tilde{S}\gamma'^2(D_1 + D_2)}{UX_2^2} \quad (3.18)$$

where $\tilde{S} = U \sum_k W_k/E_k$. The formal solution of Eq. (3.18) is

$$\sigma = \frac{\tilde{S}[\rho_0 - \gamma'^2(D_1 + D_2)/UX_2^2]}{1 + \tilde{S}}. \quad (3.19)$$

Now, from the explicit expressions for D_1 , D_2 defined in Eqs. (2.4) it can be shown that $(D_1 + D_2) \leq 0$. Thus, from Eq. (3.19) it is understood that $\sigma(\gamma' \neq 0) \geq 0$ at any temperature for $U > 0$, $\gamma' > 0$. Numerical results presented in Fig. 2(a) confirm this conclusion. As to the magnitude of anomalous density, it is seen that both kind of anisotropies lead to increasing of $|\sigma|$, which may reach even 20% of the total density of triplons for the moderate values of γ' .

In Fig. 2(b), a similar quantity, namely, the ratio of anomalous self-energy to the normal self-energy, Σ_{an}/Σ_n is presented. It is seen that Σ_{an} does not vanish even in the normal phase, where it is equal to $\Sigma_{an}(T > T_c) = \gamma$. Moreover, the presence of DM interaction changes the sign of Σ_{an} .

B. Shift in the critical temperature

The critical temperature T_c is one of the main characteristics of systems undergoing BEC transition. It is understood that the presence of any kind of interaction (or geometry of a trap) modifies the critical temperature of BEC. Quantitatively this is characterized in literature by the relative shift of critical temperature $\Delta T_c/T_c^0$ defined as

$$\frac{\Delta T_c}{T_c^0} \equiv \frac{T_c - T_c^0}{T_c^0} \quad (3.20)$$

where T_c^0 is the critical temperature of BEC transition without the interaction under consideration.

In general, the problem of accurate estimation of the shift turns out to be highly non-trivial, since close to the phase transition, the physics in the interacting gas is governed by strong fluctuations, which make perturbation theory inapplicable[29]. Nevertheless, one can find in the literature some analytical formulas for $\Delta T_c/T_c^0$ due to interparticle contact interaction[30], due to the trap geometry[31], or due to disorder[32, 33]. We now consider how the critical temperature T_c of triplon BEC may be affected by anisotropies. To find an answer to this question we have to make numerical analysis, since obtaining analytical estimations turns out to be rather complicated.

In Figs. 3(a) and (b) we present the dependence of the shift due to EA and DM interactions, respectively. For weak anisotropies these can be approximated in powers of γ/U and $\sqrt{\gamma'/U}$ as $\Delta T_c/T_c^0(\gamma) \approx a_1(\gamma/U) + a_2(\gamma/U)^2$ and $\Delta T_c/T_c^0(\gamma') \approx a'_1\sqrt{(\gamma'/U)} + a'_2(\gamma'/U)$ for

the cases of EA and DM interactions, respectively. Clearly the optimized parameters a_i and a'_i depend also on the external magnetic field H . Particularly, for TlCuCl_3 with $U = 315$ K at $H = 8.5$ T we obtained $a_1/U = 1.167 \text{ K}^{-1}$, $a_2/U^2 = -1.194 \text{ K}^{-2}$, $a'_1/\sqrt{U} = 1.647 \text{ K}^{-1/2}$ and $a'_2/U = 0.053 \text{ K}^{-1}$, as illustrated in Fig. 3.

Firstly, one may note that in both cases $\Delta T_c \geq 0$, which means that presence of the anisotropies shift the critical temperature of BEC transition, (or a crossover in the case of DM anisotropy) toward higher values. Secondly, it is seen that the influence of anisotropy is not negligibly small at moderate values of the intensities. For instance, DM interaction with $\gamma' \approx 0.1$ K modifies T_c with $\Delta T_c/T_c^0(\gamma' = 0.1 \text{ K}) \sim 50\%$. Thirdly, DM anisotropy modifies the critical temperature more strongly than EA anisotropy. For example, for the equal values of intensities, say, $\gamma = \gamma' \approx 0.1$ K, the shift due to DM interaction is nearly five times larger than due to EA interaction. Thus, the critical temperature is more sensitive to DM interaction than to EA.

C. Magnetization

In Figs. 4 the uniform magnetization $M(T)$ and $M_{\perp}^2(T)$ are presented for various values of γ and γ' as a function of temperature. It is seen that the EA interaction modifies both of these quantities mainly at low temperatures ($T \leq T_c$) (Figs. 4(a), (c)). As to the DM interaction its effect is twofold. At low temperatures it enhances M as well as M_{\perp} and in contrast to EA interaction, it prevents the staggered magnetization from vanishing at $T \geq T_c$. Thus, taking into account of DM anisotropy, at least in the linear form as in Eq. (1.2) within MFA, is inevitable in the accurate description of experimental data on M_{\perp} , reported by Tanaka *et al.*[34].

D. Heat capacity at constant field C_H

In the presence of BEC the heat capacity exhibits the following specific features.

- Its dependence on temperature has a well known λ -shape[35] which was first observed in superfluid helium[36].
- Near absolute zero, $C_V(T)$ behaves like $C_V(T) \propto T^3$, due to a linear energy dispersion, responsible for the superfluidity.

- Near the critical temperature C_V has a discontinuity, i.e., $\Delta C_V \equiv \lim_{\epsilon \rightarrow 0} [C_V(T_c - \epsilon) - C_V(T_c + \epsilon)] \neq 0$ which is expected for a second order phase transition[37].

In the present work to study these features of the heat capacity of triplons at constant magnetic field and in the presence of anisotropies, we evaluate $C_H(T)$ for the case of only EA anisotropy, (see Fig.5(a))². Firstly, it is seen that in both cases of low and high temperatures, behavior of $C_H(T)$ is not modified significantly, almost coinciding with the case without anisotropy (solid lines in Fig. 5(a)). That is the anisotropies are prominent mainly in the critical region. Further, EA interaction leaves the famous λ -shape almost unchanged (Fig. 5(a)). Actually, in the presence of EA anisotropy, there is a definite point T_c where $\rho_0(T = T_c) = 0$, which separates BEC and normal phases. This leads to a sharp maximum in the specific heat (see Fig.5(a)), as in the case of a pure BEC without any anisotropy (solid line in Fig. 5(a)). In order to find the shift in ΔC_H due to the EA interaction we evaluated ΔC_H as a function of the strength of EA interaction using Eqs. (A.8b), (A.11) and (A.14). The results are presented in Fig. 5(b). It is seen that $\Delta C_H(\gamma = 0, \gamma' = 0) \approx 0.01$ i.e., the discontinuity is positive for a pure BEC, as it is expected[35, 38]. For small values of the EA strength, $0 < \gamma \leq 0.1$ K, the function $\Delta C_H(\gamma)$ can be approximated (dashed line in Fig. 5 (b)) by $\Delta C_H(\gamma) \sim b + a\gamma$. For example, at $H = 8.5$ T, the optimal values are: $b \approx 0.01$ and $a = 0.055$ K⁻¹. In spite of the presence of EA anisotropy, ΔC_H remains finite which proves that the corresponding BEC-like transition may be classified as a second order phase transition. From Fig. 5(b) it is seen that, $\Delta C_H(\gamma)$ is always positive (upper panel), while $\Delta(dM/dT)$ remains negative for any γ . This is in a good agreement with Ehrenfest relation[39]

$$\Delta C_H = - \left\{ T \left(\frac{\partial H}{\partial T} \right) \left[\Delta \left(\frac{\partial M}{\partial T} \right) \right] \right\} \Big|_{T=T_c}. \quad (3.21)$$

IV. RESULTS FOR REALISTIC PARAMETERS FOR TICuCl₃ AND DISCUSSIONS

In the previous section we studied the effect of anisotropies on thermodynamic quantities. Particularly, we have shown that in contrast to EA interaction, DM interaction modifies their behavior dramatically. It smears BEC transition to a crossover and changes the sign of the

² C_H in the presence of DM anisotropy will be discussed in a separate paper.

anomalous density. Clearly, the significance, or measurability of such effects depend on their interaction strengths γ and γ' . Evidently, unless we have realistic values for these parameters for a real material, our studies will remain purely academic.

Among the 3D quantum dimerized magnets with a spin gap TlCuCl_3 seems to be the most experimentally studied compound[2, 4, 8, 9, 12, 40–50]. The observation of a finite M_\perp at $T \geq T_c$ [34] uniquely indicates the presence of DM interaction with a finite γ' . Thus, using existing experimental data on the magnetization and the heat capacity of TlCuCl_3 , we have made an attempt to obtain optimal values of input parameters of the present approach. The result for $H//b$ is as follows. $g = 2.06$, $U = 367$ K, $\gamma = 0.05$ K and $\gamma' = 0.0201$ K. The magnetizations M and M_\perp corresponding to this set of parameters are depicted in Figs. 6(a) and (b), respectively. It is seen that the inclusion of DM anisotropy gives a good description of the staggered magnetization especially at higher temperatures (see, inset of Fig. 6(b)). Moreover, taking into account the anomalous density σ leads to a better description of M e.g., at low temperatures, compared with approximation suggested in Ref. [28], where σ has been neglected.

Remarkably, the experimental fit of parameters can be reached with rather small values of anisotropies, namely $\gamma/U = 1.36 \times 10^{-4}$ and $\gamma'/U = 5.47 \times 10^{-5}$. In order to compare C_H with existing experimental data, one needs to perform calculations in the presence of both kinds of anisotropies and solve the problem concerning the extraction of a phonon contribution from experimental curves. This rather complicated task will be the subject of our separated paper.

Thus we have found that, the experimental data on magnetization of TlCuCl_3 can be well described by the present approach. On the other hand there exist experimental measurements on the energy of magnetic excitations. In the following subsection we shall compare our results with these experiments.

A. Energy dispersion

As it has been outlined in the Introduction, a spin gapped quantum magnet e.g., TlCuCl_3 has a dimer structure and a finite energy gap at zero field Δ_{ST} between the singlet $S = 0$ ground state and the first excited states $S = 1$. When an external field is applied and reaches a critical value $H_c = \Delta_{ST}/g\mu_B$ the gap is closed due to the Zeeman effect, as it

is illustrated in Fig. 7(a). The excitation spectrum of this compound so far was studied in detail by inelastic neutron scattering (INS)[44–49] as well as ESR measurements[12, 50].

The INS studies confirmed that the system becomes quantum critical at $H_c \approx 5.7$ T where the energy of the lowest Zeeman-split excitation $|1, -1\rangle$ crosses the nonmagnetic ground state $|0, +0\rangle$. Above this lowest mode the system remains in a gapless Goldstone mode and develops a linear dependence on the momentum, which is a good signal of occurrence of BEC. On the other hand, ESR study on this compound gave evidence for a tiny spin gap with minimal value $\Delta_{an} \sim 0.2$ meV, which was not observed in INS experiments (see Fig. 7(a)). Therefore, the experimental situation on the energy spectrum of TlCuCl_3 has not been totally clear. In fact, on the one hand, the lowest excitation spectrum for $H_c \leq H \leq H_{saturation}$ at $T \leq T_c$ is gapless, $\Delta_{an}(INS) = 0$, on the other hand, it has a finite gap $\Delta_{an}(ESR) \neq 0$ and hence can not be linear. Theoretically, it is clear that if the gap remains finite it may be caused by a lattice anisotropy. Here for clarity, it should be noted that in the present version of mean-field theory one should distinguish two types of energy dispersions. A bare dispersion $\varepsilon_k \sim k^2/2m$ and the dispersion of collective excitations, given as $E_k = \sqrt{\varepsilon_k + X_1}\sqrt{\varepsilon_k + X_2}$, where the self-energies X_1 and X_2 are discussed in Section II. The dispersion of elementary excitations at zero field ε_k is well studied experimentally[45, 47] and presented as a function of momentum and intra (inter)-dimer interactions J_i as $\varepsilon_k(J_i)$. One can find in the literature an explicit expression for $\varepsilon_k(J_i)$ with its optimized parameters[4, 9, 47], which has also been used in the present work with the normalization $\varepsilon_k|_{k \rightarrow 0} = \vec{k}^2/2m$ [39].

As to the energy spectrum at $H \geq H_c$, it is clearly model dependent. For example, in the isotropic case for $T \leq T_c$ it is gapless, given by $E_k = \sqrt{\varepsilon_k + X_1}\sqrt{\varepsilon_k} \sim ck + \mathcal{O}(k^3)$, thus, $\Delta_{an} = E_k|_{k \rightarrow 0} = 0$ in agreement with experimental results by Rüegg *et al.*[44]. In the presence of anisotropies it has a finite gap $\Delta_{an} = \sqrt{X_1 X_2}$, where X_1 and X_2 are defined by Eqs. (2.12) and (2.13). Using our optimal input parameters we obtained a finite but rather small value $\Delta_{an}(H = 14 \text{ T}, T=1.5 \text{ K})=10^{-4}$ meV, which is consistent with INS measurements, but not with ESR: $\Delta_{an}(H = 14 \text{ T}, T=1.5 \text{ K})=0.2$ meV[12, 50]. In Fig. 7(b) we present quasiparticle spectrum $E_k = \sqrt{\varepsilon_k + X_1}\sqrt{\varepsilon_k + X_2}$, ($k_x = k_z = 0, k_y = \pi q_y$) for $H = 14$ T at $T = 1.5$ K. It is seen that, the excitation energy in the present approximation is almost linear, in accordance with experimental results. However, the experimental values of E_k^{exp} are rather underestimated. This can be understood as follows. As it has been shown in

Section II at low temperatures the self-energies, especially X_1 is rather small (Fig. 1). Our input parameters optimized by experimental magnetizations lead to much smaller values: $X_1(H = 14 \text{ T}, T=1.5 \text{ K})=0.67 \times 10^{-5} \text{ K}$, $X_2(H = 14 \text{ T}, T=1.5 \text{ K})=0.19 \text{ K}$, thus $X_1 \ll X_2$. As a result, the momentum dependence of the dispersion is similar to that of isotropic one, $E_k = \sqrt{\varepsilon_k + X_1} \sqrt{\varepsilon_k + X_2} \sim \sqrt{\varepsilon_k} \sqrt{\varepsilon_k + X_2}$ which is practically nothing but the Goldstone mode. Thus, we may come to the conclusion that in accordance with present approximation the lowest excitation energy of TlCuCl_3 at very low temperatures has a rather small, but finite gap and exhibits, practically, a linear dispersion at small momentum, in spite of the presence of EA and DM interactions. Note that, a similar situation has been observed for compounds $\text{Sr}_3\text{Cr}_2\text{O}_8$ and $\text{Ba}_3\text{Cr}_2\text{O}_8$ which have DM interaction, but no anisotropy gap, i.e., $\Delta_{an}(\text{Sr}_3\text{Cr}_2\text{O}_8)=0$, $\Delta_{an}(\text{Ba}_3\text{Cr}_2\text{O}_8)=0$. [10]

B. Discussions

In the present section, having fixed the parameters of the theory by magnetization data on TlCuCl_3 , we have studied its energy spectrum above the critical field at $T \leq 1.5 \text{ K}$. We have found that the description of magnetizations for $H//b$ is quite good, while that of the energy dispersion of the low-lying magnetic excitations needs to be improved. In some sense, this brings to mind the situation in nuclear physics: one can choose optimal parameters for the nucleon-nucleon potential by experimental data on cross sections, but fails to accurately describe the binding energies of light nuclei. Anyway, the main reason of our failure seems to be the simplicity of the Hamiltonian H_{DM} used here (the last term in Eq. (1.2)). In fact, in deriving this linear Hamiltonian it has been assumed that, the DM vector is parallel to x , i.e., $\vec{D} = [D_x, 0, 0]$ [17]. Therefore, it is naturally expected that by using a more general form for H_{DM} , where other components of \vec{D} are also included [16, 24] one will be able to describe not only magnetizations, but also excitation energies in the extended version of the present mean-field approach. Note that, by neglecting the other components of the DM vector, one cannot describe magnetizations for $H \perp (1, 0, \bar{2})$ either.

V. SUMMARY AND CONCLUSIONS

We have studied effects of lattice anisotropies on thermodynamic characteristics of spin-gapped quantum magnets for $H_c \leq H < H_{Saturation}$ by applying our extended mean-field based approach, proposed in our previous work[22]. This nonperturbative approach takes into account the anomalous density and both EA and DM interactions more accurately than it is done e.g., in the HFP approximation. We derived explicit expressions for some thermodynamic quantities which include the self-energies X_1 and X_2 , and the condensate fraction ρ_0 . Analysis of the coupled equations with respect to these three quantities show that at high temperatures $T \gg T_c$, the self-energies $X_{1,2}$ are not significantly affected by EA and DM interactions. Meanwhile, the latter strongly modifies the condensate fraction converting BEC transition into a crossover.

At low temperatures the DM interaction increases ρ_0 , but leads to rather small values of X_1 , compared with the isotropic case. As a result, the energy dispersion $E_k = \sqrt{(\varepsilon_k + X_1)(\varepsilon_k + X_2)}$, develops a linear dependence at small momentum, in accordance with experimental measurements.

In contrast to EA interaction, the presence of DM interaction, even in the simple linear form in the Hamiltonian, modifies the anomalous density, changing its sign. Particularly, it is expected that, the usual “ λ -shape” of the heat capacity disappears due to strong DM interactions. On contrary, the presence of only EA anisotropy leaves the “ λ -shape” of the heat capacity unchanged. The discontinuity in C_H close to the critical temperature is shifted significantly for moderate values of the intensity of the exchange anisotropy.

We have found optimal input parameters of the Hamiltonian for the compound TlCuCl_3 which describes experimental data on magnetizations, at least for $H//b$, quite well. This set of parameters lead to a linear dispersion of energy of quasiparticles, but predicts a fairly small value of an anisotropy gap, estimated by ESR measurements.

In future work we plan to extend our Hamiltonian by taking into account a more realistic DM interaction to obtain better description of experimental data on the spectrum of low lying excitations, as well as the heat capacity.

Acknowledgements

We are indebted to Andreas Schilling for useful discussions and comments. AR acknowledges support by TUBITAK-BIDEB (2221), AK is supported by the Ministry of Innovative Development of the Republic of Uzbekistan and thankful to group of J. Osterwalder at Physics Institute of University of Zurich. BT is supported by Science and Technological Council of Turkey (TUBITAK) under Grant No: 119N689 and Turkish Academy of Sciences (TUBA) under Grant No. AD21. This work is partly supported by funding from Academy of Sciences of the Republic of Uzbekistan.

Appendix A: Explicit expressions for some thermodynamic parameters

As shown in Section II the physics of the cases with and without anisotropies are quite different. In the presence of DM interaction all useful expressions for physical observables may be found by setting $\xi = i$ in Eqs. (2.3a) and (2.3b) which are to be solved with the restrictions $X_1 \geq 0$, $X_2 \geq 0$. However, when DM is absent ($\gamma' = 0, \gamma \neq 0$), one must be aware of the Hugenholtz-Pines (HP) theorem[51] which holds in the limit $\gamma \rightarrow 0$. Below, we discuss these two cases separately.

1. Mode 1: $\gamma' = 0, \gamma \neq 0$

We start from the explicit expression for Ω ,

$$\begin{aligned} \Omega(\gamma' = 0, \gamma \neq 0, \xi = 1) &= U\rho_1^2 + \frac{U(\sigma^2 + \rho_0^2)}{2} + \rho_1 \left(-\frac{X_1}{2} - \frac{X_2}{2} - \mu + 2U\rho_0 \right) + \\ &\quad \sigma \left(\frac{X_2}{2} - \frac{X_1}{2} + \gamma + U\rho_0 \right) + \gamma\rho_0 - \mu_0\rho_0 + \Omega_T \end{aligned} \quad (\text{A.1})$$

where

$$\Omega_T = \frac{1}{2} \sum_k (E_k - \varepsilon_k) + T \sum_k \ln(1 - e^{-\beta E_k}) \quad (\text{A.2a})$$

$$X_1 = U(3\rho_0 + 2\rho_1 + \sigma) - \mu + \gamma \quad (\text{A.2b})$$

$$X_2 = U(\rho_0 + 2\rho_1 - \sigma) - \mu - \gamma \quad (\text{A.2c})$$

$$E_k = \sqrt{(\varepsilon_k + X_1)(\varepsilon_k + X_2)} \quad (\text{A.2d})$$

and $\mu_0 = 2U\rho_1 + U\sigma + \gamma + U\rho_0$ is introduced to avoid the Hohenberg-Martin dilemma[52] in the condensate phase. In this phase, $\rho_0(T \leq T_c) = 0$ and HP relation may be written in a slightly “broken” form[25]:

$$\Sigma_n - \Sigma_{an} - \mu = X_2 = 2\gamma \quad (\text{A.3})$$

which gives a gapless energy dispersion in the $\gamma \rightarrow 0$ limit: $E_k(T < T_c) = \sqrt{(\varepsilon_k + X_1)(\varepsilon_k + 2\gamma)}$. Using (A.2b), (A.2c) and (A.3) yields

$$X_1(T \leq T_c) = 2U\sigma + 2U\rho_0 + 4\gamma, \quad X_2(T \leq T_c) = 2\gamma \quad (\text{A.4})$$

whose solution is positive definite due to $|\rho_0| \geq |\sigma|$. This equation may be rewritten in a more convenient form as

$$\Delta = \frac{X_1}{2} = \mu + 2U(\sigma - \rho_1) + 5\gamma \quad (\text{A.5})$$

where σ and ρ_1 are given by Eqs. (2.6a) and (2.6b) with $X_2 = 2\gamma$, $X_1 = 2\Delta$ and $\mu = g\mu_B(H - H_c)$. Having solved Eq. (A.5) with respect to Δ one may evaluate the densities as

$$\rho_0 = \frac{\Delta - 2\gamma - U\sigma}{U}, \quad (\text{A.6a})$$

$$\rho = \frac{\Delta + \mu + \gamma}{2U}. \quad (\text{A.6b})$$

In the normal phase ($T > T_c$), one may neglect ρ_0 in Eqs. (A.2b) and (A.2c) to obtain

$$X_{1,2}(T > T_c) = 2U\rho - \mu \pm \gamma \pm \sigma \quad (\text{A.7a})$$

$$\rho(T > T_c) = \sum_k \frac{1}{e^{\beta\omega_k} - 1} \quad (\text{A.7b})$$

$$\omega_k = \sqrt{(\varepsilon_k + X_1)(\varepsilon_k + X_2)}. \quad (\text{A.7c})$$

The entropy S , heat capacity C_H , and Grüneisen parameter may be found as[53, 54]

$$S = - \left(\frac{\partial \Omega}{\partial T} \right)_H = - \sum_k \ln [1 - \exp(-\beta \mathcal{E}_k)] + \beta \sum_k \frac{\mathcal{E}_k}{e^{\beta \mathcal{E}_k} - 1} \quad (\text{A.8a})$$

$$C_H = T \left(\frac{\partial S}{\partial T} \right) = \frac{1}{4} \sum_k W'_k \mathcal{E}_k (\mathcal{E}'_{k,T} - \beta \mathcal{E}_k) \quad (\text{A.8b})$$

$$\Gamma_H = - \frac{1}{C_H} \left(\frac{\partial \mu}{\partial T} \right)_H = \frac{g\mu_B}{C_H} \left(\frac{\partial \rho}{\partial T} \right) \quad (\text{A.8c})$$

where $\mathcal{E}_k = \sqrt{(\varepsilon_k + X_1)(\varepsilon_k + X_2)}$, $\mathcal{E}'_{k,T} = (\partial \mathcal{E}_k / \partial T)_H$ and $X_{1,2}$ are given by Eqs. (A.4) and (A.7a). Below we give explicit expressions for $\mathcal{E}'_{k,T}$ and ρ'_T for normal ($T > T_c$) and BEC ($T \leq T_c$) phases where the critical temperature is defined at the point $\rho_0(T = T_c) = 0$.

a. Critical temperature and density

The condition $\rho_0(T = T_c) = 0$ leads the following coupled equations with respect to T_c and σ_c [25]:

$$\frac{\mu}{2U} + \frac{\sigma_c + 3\tilde{\gamma}}{2} - \sum_k \frac{f_b(E_k^c)}{E_k^c} [\varepsilon_k + U(\sigma_c + 3\tilde{\gamma})] = 0 \quad (\text{A.9})$$

$$\sigma_c + U(\sigma_c + \tilde{\gamma}) \sum_k \frac{f_b(E_k^c)}{E_k^c} = 0$$

where $E_k^c = E_k(T \rightarrow T_c) = \sqrt{\varepsilon_k + X_1^c} \sqrt{\varepsilon_k + 2\tilde{\gamma}}$, $X_1^c = 2U(\sigma_c + 2\tilde{\gamma})$, $f_b(x) = 1/(\exp(x/T_c) - 1)$ and $\tilde{\gamma} = \gamma/U$. The critical density is given by

$$\rho(T = T_c) = \frac{\mu}{2U} + \frac{\sigma_c + 3\tilde{\gamma}}{2} \equiv \rho_c. \quad (\text{A.10})$$

b. Normal phase

For $T > T_c$, differentiating Eq. (A.7b) and using Eq. (A.7c) we obtain following set of equations:

$$\begin{aligned}
\rho'_T(T > T_c) &= \frac{b_1 a_{22} - b_2 a_{12}}{a_{11} a_{22} - a_{12} a_{21}}, & \sigma'_T(T > T_c) &= \frac{b_2 a_{11} - b_1 a_{21}}{a_{11} a_{22} - a_{12} a_{21}}, \\
\frac{d\omega_k}{dT} &= \frac{U}{\omega_k} [2(\varepsilon_k - \mu + 2U\rho)\rho'_T - U(\tilde{\gamma} + \sigma)\sigma'_T], \\
a_{11} &= 1 - 2A + \frac{U}{2} \sum_k \frac{(\varepsilon_k - \mu + 2U\rho)^2 (-2 + 4W_k - \omega_k W'_k)}{\omega_k^3}, \\
a_{12} &= \frac{U^2}{4} \sum_k \frac{(\varepsilon_k - \mu + 2U\rho)(\sigma + \tilde{\gamma})(2 - 4W_k + \omega_k W'_k)}{\omega_k^3}, \\
a_{22} &= 1 - \frac{U^3}{4(1+A)^2} \sum_k \frac{\tilde{\gamma}(\sigma + \tilde{\gamma})(2 - 4W_k + \omega_k W'_k)}{\omega_k^3}, \\
a_{21} &= \frac{2\tilde{\gamma}a_{12}}{(1+A)^2(\sigma + \tilde{\gamma})}, & b_1 &= -\frac{1}{4T} \sum_k (\varepsilon_k - \mu + 2U\rho)W'_k, \\
b_2 &= \frac{U\tilde{\gamma}}{4T(1+A)^2} \sum_k W'_k, & A &= U \sum_k \frac{1}{\omega_k(\exp(\beta\omega_k) - 1)},
\end{aligned} \tag{A.11}$$

where $W'_k = -\beta/\sinh^2(\beta\omega_k/2)$ and $W_k = 1/2 \coth(\beta\omega_k/2)$.

c. BEC phase

In this case $\mathcal{E}_k(T) = E_k(T) = \sqrt{(\varepsilon_k + 2\Delta(T))(\varepsilon_k + 2\gamma)}$ differentiation of which gives

$$\mathcal{E}'_{k,T} = E'_{k,T} = \frac{\varepsilon_k + 2\gamma}{E_k} \Delta'_T. \tag{A.12}$$

To find $\Delta'_T = (\partial\Delta/\partial T)$, we can differentiate both sides of Eq. (A.5) with respect to T and solve it for Δ'_T . The result is

$$\Delta'_T = \left(\frac{\partial\Delta}{\partial T} \right)_H = \frac{US_3}{2T(2S_4 + 1)} \tag{A.13}$$

with $S_3 = \sum_k W'_k(\varepsilon_k + 2\Delta)$ and $S_4 = U \sum_k (4W_k + E_k W'_k)/4E_k$. As to ρ'_T it can be found directly from (A.6b) as

$$\rho'_T(T \leq T_c) = \frac{S_3}{4T(2S_4 + 1)}. \quad (\text{A.14})$$

At last, setting in Eqs. (A.11) and (A.14) $\rho_0 = 0$, $T = T_c$, $E_k = \omega_k = \sqrt{\varepsilon_k + X_1^c} \sqrt{\varepsilon_k + 2\gamma}$ one may define the cusp in ρ'_T as $\Delta\rho'_T = \rho'_T(T_c^-) - \rho'_T(T_c^+)$ presented in Fig.5b. As to the cusp in C_H , presented also in Fig.5b may be found in a similar way from Eq.s (A.8b), (A.11) and (A.14).

2. Mode 2: $\gamma' \neq 0, \gamma \neq 0$ case

The expressions for S , C_H , and Γ_H remain formally unchanged. However, explicit expressions for $\mathcal{E}'_{k,T}$ and $\partial\rho/\partial T$ in Eq. (A.8b) and (A.8c) are quiter complicated. Implicit differentiation of $E_k = \sqrt{(\varepsilon_k + X_1(T))(\varepsilon_k + X_2(T))}$ gives

$$\mathcal{E}'_{k,T} = \frac{\partial E_k}{\partial T} = \frac{(\varepsilon_k + X_2)X'_1 + (\varepsilon_k + X_1)X'_2}{2E_k} \quad (\text{A.15})$$

where $X'_1 = \partial X_1/\partial T$ and $X'_2 = \partial X_2/\partial T$ whose explicit expressions will be given below. Now, differentiating both sides of equations $\rho_1 = (A+B)/2$ and $\sigma = (B-A)/2$ with respect to temperature one obtains

$$\frac{d\rho_0}{dT} = C_\rho[X'_1(B'_1 + 3A'_1) + X'_2(A'_1 + 3A'_2) + A'_t + B'_t] \quad (\text{A.16a})$$

$$\frac{d\rho_1}{dT} = \frac{X'_1}{2}(A'_1 + B'_1) + \frac{X'_2}{2}(A'_1 + A'_2) + \frac{1}{2}(A'_t + B'_t) \quad (\text{A.16b})$$

$$\frac{d\sigma}{dT} = \frac{X'_1}{2}(B'_1 - A'_1) + \frac{X'_2}{2}(A'_1 - A'_2) + \frac{1}{2}(B'_t - A'_t) \quad (\text{A.16c})$$

$$\frac{d\rho}{dT} = \frac{d\rho_0}{dT} + \frac{d\rho_1}{dT} \quad (\text{A.16d})$$

where $C_\rho = -U\rho_0^{3/2}/(\gamma' + 2U\rho_0^{3/2})$, $A'_t = -(\beta/4) \sum_k W'_k(\varepsilon_k + X_1)$, $B'_t = -(\beta/4) \sum_k W'_k(\varepsilon_k + X_2)$ and $A'_i = \partial A/\partial X_i$, $B'_i = \partial B/\partial X_i$ given in Eq. (2.4e).

In the above equations $X'_1 = dX_1/dT$ and $X'_2 = dX_2/dT$ are still unknown. To find them we rewrite Eq. (29a) and (29b) in our previous paper[22] in the following equivalent form

$$M_{11}A'_1 + M_{12}B'_1 = 0 \quad (\text{A.17})$$

$$M_{12}A'_1 + M_{11}A'_2 + \frac{2\gamma'^2}{X_2^2} = 0 \quad (\text{A.18})$$

with $M_{11} = -X_2 + 2U\rho_0 + \gamma'/\sqrt{\rho_0}$, $M_{12} = -X_1 + 2U\sigma + 2\gamma + \gamma'/\sqrt{\rho_0}$.

Now, differentiating both sides of Eq. (A.17) and (A.18) and solving the resulting equations for X'_1 and X'_2 one finally gets

$$X'_1 = \frac{A_{12}b_2 - b_1A_{22}}{A_{11}A_{22} - A_{21}A_{12}}, \quad X'_2 = \frac{A_{21}b_1 - b_2A_{11}}{A_{11}A_{22} - A_{21}A_{12}} \quad (\text{A.19})$$

where

$$A_{11} = A'_1M_{11,1} + M_{11}A''_{11} + B'_1(-1 + M'_{12,2}) + M_{12}B''_{11} \quad (\text{A.20a})$$

$$A_{12} = A'_1(-1 + M'_{11,1}) + M_{11}A''_{12} + M'_{12,2}B'_1 + M_{12}A''_{11} \quad (\text{A.20b})$$

$$A_{21} = A'_1(-1 + M'_{12,2}) + M_{12}A''_{11} + M'_{11,1}A'_2 + M_{11}A''_{12} \quad (\text{A.20c})$$

$$A_{22} = A'_1M'_{12,2} + M_{12}A''_{12} + (-1 + M'_{11,1})A'_2 + M_{11}A''_{12} \quad (\text{A.20d})$$

$$b_1 = M'_{11,t}A'_1 + M_{11}A''_{1,t} + M'_{12,t}B'_1 + M_{12}B''_{1,t} \quad (\text{A.20e})$$

$$b_2 = M'_{12,t}A'_1 + M_{12}A''_{1,t} + M'_{11,t}A'_2 + M_{11}A''_{2,t} \quad (\text{A.20f})$$

and we have introduced the abbreviations $M'_{ij,k} = \partial M_{ij}/\partial X_k$ and $A''_{ij} = \partial^2 A/\partial X_i \partial X_j$. f'_t is an explicit derivative with respect to temperature $f'_t(\varphi(X_1(T), X_2(T), T)) = df/dT - (\partial f/\partial \varphi)X'_1 - (\partial f/\partial \varphi)X'_2$.

References

-
- [1] V. Zapf, M. Jaime, and C. D. Batista, *Bose-Einstein condensation in quantum magnets*, Rev. Mod. Phys. **86** (2014) 563.
 - [2] E. Ya. Sherman, P. Lemmens, B. Busse, A. Oosawa, and H. Tanaka, *Sound Attenuation Study on the Bose-Einstein Condensation of Magnons in $TlCuCl_3$* , Phys. Rev. Lett. **91** (2003) 057201.
 - [3] X.-G. Zhou, Yuan Yao, Y.H. Matsuda, A. Ikeda, A. Matsuo, K. Kindo, and H. Tanaka, *Particle-Hole Symmetry Breaking in a Spin-Dimer System $TlCuCl_3$ Observed at 100 T* Phys. Rev. Lett. **125**, (2020) 267207.
 - [4] M. Matsumoto, B. Normand, T. M. Rice, and M. Sigrist, *Magnon Dispersion in the Field-Induced Magnetically Ordered Phase of $TlCuCl_3$* , Phys. Rev. Lett. **89** 077203.
 - [5] V.I. Yukalov *Difference in Bose-Einstein condensation of conserved and unconserved particles*, Laser Phys. **22** (2012) 1145.

- [6] J. O. Andersen, *Theory of the weakly interacting Bose gas*, Rev. Mod. Phys. **76** (2004) 599.
- [7] N. Cavadini, W. Henggeler, A. Furrer, H. U. Güdel, K. Krämer, and H. Mutka, *Magnetic excitations in the quantum spin system $KCuCl_3$* , Eur. Phys. J. B **7** (1999) 519.
- [8] M. Matsumoto, B. Normand, T. M. Rice, and M. Sigrist, *Field- and pressure-induced magnetic quantum phase transitions in $TlCuCl_3$* , Phys. Rev. B **69** (2004) 054423.
- [9] G. Misguich, and M. Oshikawa, *Bose-Einstein Condensation of Magnons in $TlCuCl_3$: Phase Diagram and Specific Heat from a Self-consistent Hartree-Fock Calculation with a Realistic Dispersion Relation*, J. Phys. Soc. Jpn. **73** (2004) 3429.
- [10] Zhe Wang, D. Kamenskyi, O. Capas, M. Schmidt, D. L. Quintero-Castro, A. T. M. N. Islam, B. Lake, A. A. Aczel, H. A. Dabkowska, A. B. Dabkowski, G. M. Luke, Yuan Wan, A. Loidl, M. Ozerov, J. Wosnitza, S. A. Zvyagin, and J. Deisenhofer, *High-field electron spin resonance spectroscopy of singlet-triplet transitions in the spin-dimer systems $Sr_3Cr_2O_8$ and $Ba_3Cr_2O_8$* , Phys. Rev. B **89** (2014)174406.
- [11] A. K. Kolezhuk, V. N. Glazkov, H. Tanaka, and A. Oosawa, *Dynamics of an anisotropic spin dimer system in a strong magnetic field*, Phys. Rev. B **70** (2004) 020403(R).
- [12] V. N. Glazkov, A. I. Smirnov, H. Tanaka, and A. Oosawa, *Spin-resonance modes of the spin-gap magnet $TlCuCl_3$* , Phys. Rev. B **69** (2004) 184410.
- [13] V. N. Glazkov, T. S. Yankova, J. Sichelschmidt, D. Huvonen and A. Zheludev, *Electron spin resonance study of anisotropic interactions in a two-dimensional spin-gap magnet $(C_4H_{12}N_2)(Cu_2Cl_6)$* , Phys. Rev. B **85** (2012) 054415.
- [14] K.Yu. Povarov, A. I. Smirnov, O. A. Starykh, S.V. Petrov and A.Ya. Shapiro *Modes of Magnetic Resonance in the Spin-Liquid Phase of Cs_2CuCl_4* , Phys. Rev. Lett. **107** (2011) 037204 .
- [15] S. A. Zvyagin, J. Wosnitza, C. D. Batista, M. Tsukamoto, N. Kawashima, J. Krzystek, V. S. Zapf, M. Jaime, N. F. Oliveira, Jr., and A. Paduan-Filho *Magnetic Excitations in the Spin-1 Anisotropic Heisenberg Antiferromagnetic Chain System DTN* , Phys. Rev. Lett. **98** (2007) 047205 .
- [16] S. Miyahara, F. Mila, K. Kodama, M. Takigawa, M. Horvatic, C. Berthier, H. Kageyama, and Y. Ueda, *The effects of intra-dimer Dzyaloshinsky-Moriya interaction on the properties of $SrCu_2(BO_3)_2$ in an external magnetic field*, J. Phys.: Condens. Matter **16** (2004) 911.
- [17] J. Sirker, A. Weisse, and O. P. Sushkov, *Consequences of spin-orbit coupling for the Bose-*

- Einstein condensation of magnons*, Europhys Lett. **68** (2004) 275.
- [18] A. Rakhimov, S. Mardonov, and E.Ya.Sherman, *Macroscopic properties of triplon Bose-Einstein condensates*, Ann. Phys. **326** (2011) 2499.
- [19] F. Cooper, B. Mihaila, J. F. Dawson, C.-C. Chien, and E. Timmermans, *Auxiliary-field approach to dilute Bose gases with tunable interactions*, Phys. Rev. A **83** (2011) 053622.
- [20] H. Kleinert and V. Schulte-Frohlinde, *Critical Properties of ϕ^4 -Theories* (Singapore: World Scientific) (2001).
- [21] A. Rakhimov, C. K. Kim, S.-H. Kim, and J. H. Yee, *Stability of the homogeneous Bose-Einstein condensate at large gas parameter*, Phys. Rev. A **77** (2008) 033626.
- [22] A. Rakhimov, A. Khudoyberdiev, L. Rani, and B. Tanatar, *Spin-gapped magnets with weak anisotropies I: Constraints on the phase of the condensate wave function*, Ann.Phys 424 (2021) 168361.
- [23] S. M. Barnett, K. Burnett, J. A. Vaccaro, *Why a Condensate Can Be Thought of as Having a Definite Phase*, J Res Natl Inst Stand Technol. 101(4): (1996) 593.
- [24] M. Matsumoto, T. Shoji and M. Koga , *Theory of magnetic excitations and electron spin resonance for anisotropic spin dimer systems*, J. Phys. Soc. Japan, **77** (2008) 074712.
- [25] A. Khudoyberdiev, A. Rakhimov, and A. Schilling, *Bose-Einstein condensation of triplons with a weakly broken $U(1)$ symmetry*, New J. Phys. **19** (2017) 113002.
- [26] N. N. Bogoliubov , *On the Theory of Superfluidity*, (in English). Journal of Physics **11** (1) (1947) 23 32.
- [27] R. Lopes, C. Eigen, N. Navon, D. Clement, R. P. Smith, and Z. Hadzibabic, *Quantum depletion of a Homogeneous Bose-Einstein condensate*, Phys. Rev. Lett. **119** (2017) 190404.
- [28] J. Sirker, A. Weisse, and O. P. Sushkov, *The Field-induced magnetic ordering transition in $TlCuCl_3$* , J. Phys. Soc. Jpn. Vol. **74** (2005) 129.
- [29] V. I. Yukalov and E. P. Yukalova, *Bose Einstein condensation temperature of weakly interacting atoms*, Laser Phys. Lett. **14** (2017) 073001.
- [30] F. F. de Souza Cruz, M. B. Pinto, and R. O. Ramos, *Transition temperature for weakly interacting homogeneous Bose gases*, Phys. Rev. B **64** (2001) 014515.
- [31] P. Arnold and B. Tomasik, *T_c for trapped dilute Bose gases: A second-order result*, Phys. Rev. A **64** (2001) 053609.
- [32] A. Rakhimov, Sh. Mardonov, E. Ya. Sherman and A. Schilling, *The effects of disorder in*

- dimerized quantum magnets in mean field approximations*, New J. Phys. **14** (2012) 113010.
- [33] A. V. Lopatin and V. M. Vinokur, *Thermodynamics of the Superfluid Dilute Bose Gas with Disorder*, Phys. Rev. Lett **88** (2002) 235503.
- [34] H. Tanaka, A. Oosawa, T. Kato, H. Uekusa, Y. Ohashi, K. Kakurai, and A. Hoser, *Observation of Field-induced transverse Neel ordering in the spin gap system $TlCuCl_3$* , J. Phys. Soc. of Japan Vol. **70** (2001) 939.
- [35] K. Huang, *Statistical Mechanics*, John Wiley & Sons (1987).
- [36] R.W. Hill, O.V. Lounasmaa *The specific heat of liquid helium* - Philosophical Magazine, (1957).
- [37] L. D. Landau, E. M. Lifshitz, *Statistical Physics, 3rd ed., Part 1* Elsevier Butterworth-Heinemann, (1980).
- [38] A. Rakhimov and I. N. Askerzade, *Thermodynamics of noninteracting bosonic gases in cubic optical lattices versus ideal homogeneous Bose gases*, Int. J. Mod. Phys. B **29**, No. 18 (2015) 1550123.
- [39] A. Rakhimov, A. Gazizulina, Z. Narzikulov, A. Schilling, and E. Ya. Sherman, *Magnetocaloric effect and Grüneisen parameter of quantum magnets with a spin gap*, Phys. Rev. B **98** (2018) 144416.
- [40] R. Dell'Amore and A. Schilling, K. Krämer *Fraction of Bose-Einstein condensed triplons in $TlCuCl_3$ from magnetization data*, Phys. Rev. B, **78** (2008) 224403 .
- [41] A. Furrera and C. Rüegg, *Bose-Einstein condensation in magnetic materials*, Physica B **385** (2006) 295.
- [42] A. Oosawa, H. Aruga Katori, and H. Tanaka, *Specific heat study of the field-induced magnetic ordering in the spin-gap system $TlCuCl_3$* Phys. Rev. B **63** (2001) 134416.
- [43] A. Oosawa, M. Ishii, and H. Tanaka *Field-induced three-dimensional magnetic ordering in the spin-gap system $TlCuCl_3$* , J. Phys. Condens. Matter. **11** (1999) 265 .
- [44] Ch. Rüegg, N. Cavadini, A. Furrer, H.-U. Gudel, K. Krämer, H. Mutka, A. Wildes, K. Habicht, and P. Vorderwisch, *Bose-Einstein condensation of the triplet states in the magnetic insulator $TlCuCl_3$* , Nature **423** (2003) 62.
- [45] A. Oosawa, T. Kato, H. Tanaka, K. Kakurai, M. Müller, and H.-J. Mikeska, *Magnetic excitations in the spin-gap system $TlCuCl_3$* , Phys. Rev. B **65** (2002) 094426.
- [46] Ch. Rüegg, B. Normand, M. Matsumoto, Ch. Niedermayer, A. Furrer, K.W. Krämer, H.-U. Gudel, Ph. Bourges, Y. Sidis, and H. Mutka *Quantum Statistics of Interacting Dimer Spin*

- Systems*, Phys. Rev. Lett **95** (2005) 267201.
- [47] N. Cavadini, G. Heigold, W. Henggeler, A. Furrer, H.-U. Güdel, K. Krämer, and H. Mutka, *Magnetic excitations in the quantum spin system $TlCuCl_3$* , Phys. Rev. B **63** (2001) 172414.
- [48] N. Cavadini, Ch. Rüegg, A. Furrer, H.-U. Güdel, K. Krämer, H. Mutka, and P. Vorderwisch, *Triplet excitations in low- H_c spin-gap systems $KCuCl_3$ and $TlCuCl_3$: An inelastic neutron scattering study*, Phys. Rev. B **65** (2002) 132415.
- [49] Ch. Rüegg, N. Cavadini, A. Furrer, K. Krämer, H. U. Güdel, P. Vorderwisch, H. Mutka *Spin dynamics in the high-field phase of quantum-critical $S=1/2$ $TlCuCl_3$* , Appl. Phys. A **74** [Suppl.] (2002) S840
- [50] S. Kimuraa, M. Hagiwara, H. Tanaka, A.K. Kolezhuk, and K. Kindo , *High-field ESR measurements on the spin gap system $TlCuCl_3$* , Journal of Magnetism and Magnetic Materials **310** (2007) 1218.
- [51] N. M. Hugenholtz and D. Pines, *Ground-state energy and excitation spectrum of a System of interacting Bosons*, Phys. Rev. **116** (1959) 489.
- [52] P. C. Hohenberg and P.C. Martin *Microscopic Theory of Superfluid Helium*, Ann. Phys. **34** (1965) 291.
- [53] A. Rakhimov, M. Nishanov and B. Tanatar, *Joule-Thomson temperature of a triplon system of dimerized quantum magnets*, Phys. Lett. A **384** (2020) 126313.
- [54] A. Rakhimov, M. Nishanov ,L. Rani and B. Tanatar, *Characteristic temperatures of a triplon system of dimerized quantum magnets*, Int. J. Mod. Phys. B, **35** (2021) 2150018.

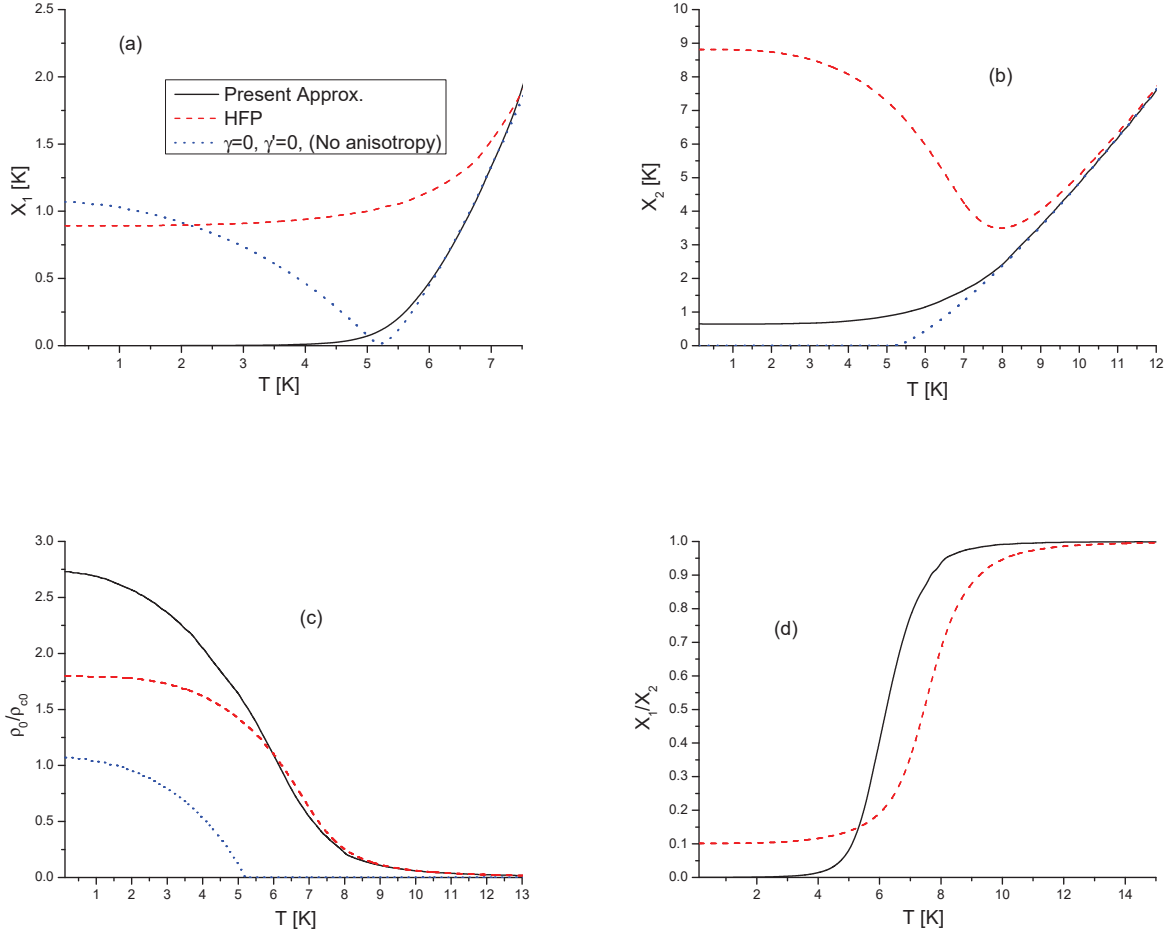


FIG. 1: Physical solutions of Eqs. (2.12) and (2.13) with only anisotropic DM interaction for the input parameters $g = 2.06$, $U = 315$ K, $H = 8.5$ T, $\gamma' = 0.1$ K, and $\gamma = 0$ as a function of temperature. The parameters of bare dispersion ε_k are taken from Ref. [9]; (a), (b) and (c) represent the self-energies $X_1(T)$, $X_2(T)$ and the condensate fraction $\rho_0(T)/\rho_{0c}$ ($\rho_{0c} = \mu/2U = 0.07$), respectively, while (d) illustrates the ratio $X_1(T)/X_2(T)$. Solid and dashed lines correspond to present approximation and that by Ref. [28], corresponding to the case with formally setting $\sigma = \gamma = (\gamma')^2 = 0$ in Eqs. (2.12) and (2.13), respectively. The dotted lines represent isotropic case with $\gamma = \gamma' = 0$.

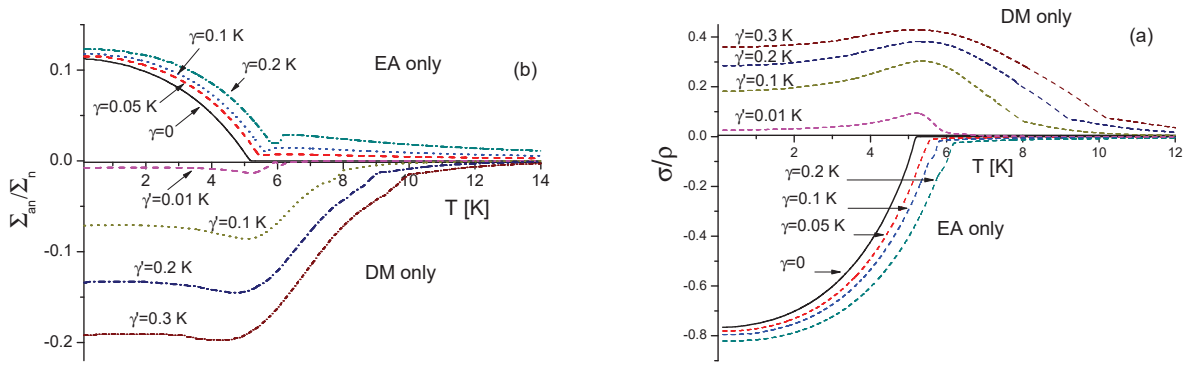


FIG. 2: (a) The ratio of anomalous density σ to the total density ρ of triplons as a function of temperature for various values of DM and EA interactions. (b) The same as in (a) but for the ratio of anomalous and normal self-energies. It is seen that the presence of DM interaction reverses the sign of both anomalous density and self-energy. The solid curves in both figures correspond to isotropic case with $\gamma = \gamma' = 0$. The input parameters are the same as in Fig. 1.

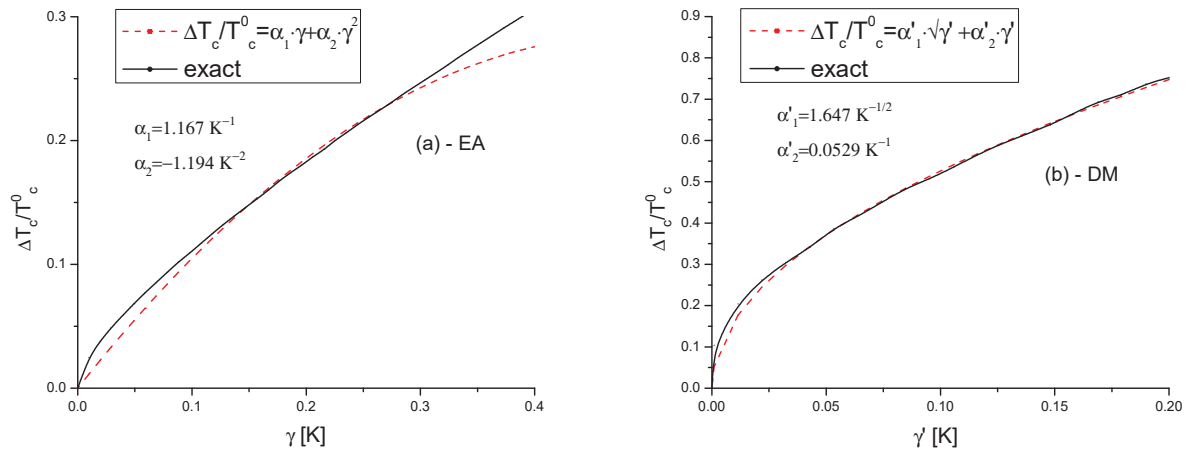


FIG. 3: The shift in critical temperature due to EA (a) and DM (b) interactions (solid curves). Dashed curves are phenomenological fits. The input parameters are the same as in Fig. 1.

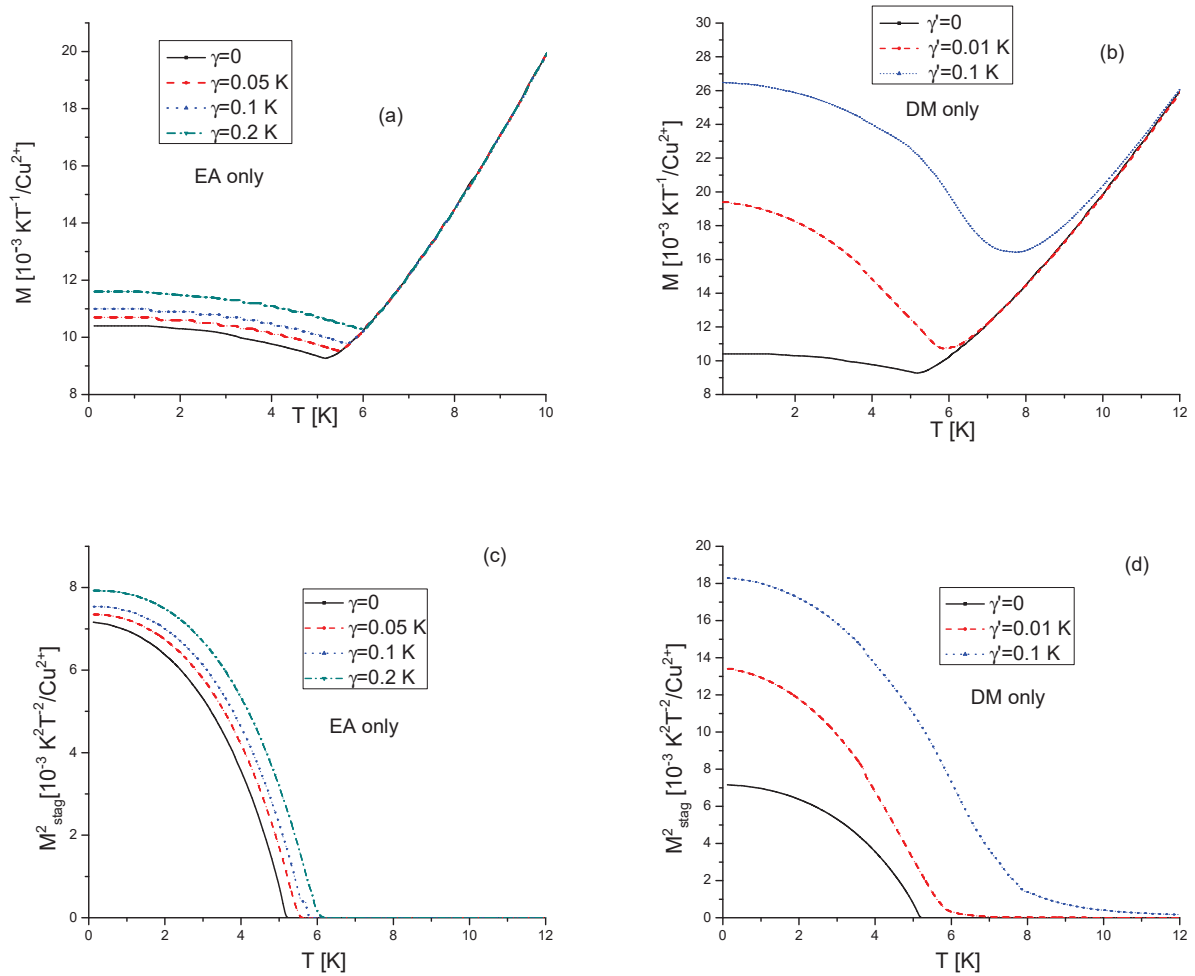


FIG. 4: Uniform magnetization as a function of temperature with only EA (a) and DM (b) anisotropies. Solid lines correspond to the isotropic case with $\gamma = \gamma' = 0$. (c) and (d) display the square of staggered magnetization $(M_{\perp})^2$. The input parameters are the same as in Figs. 1.

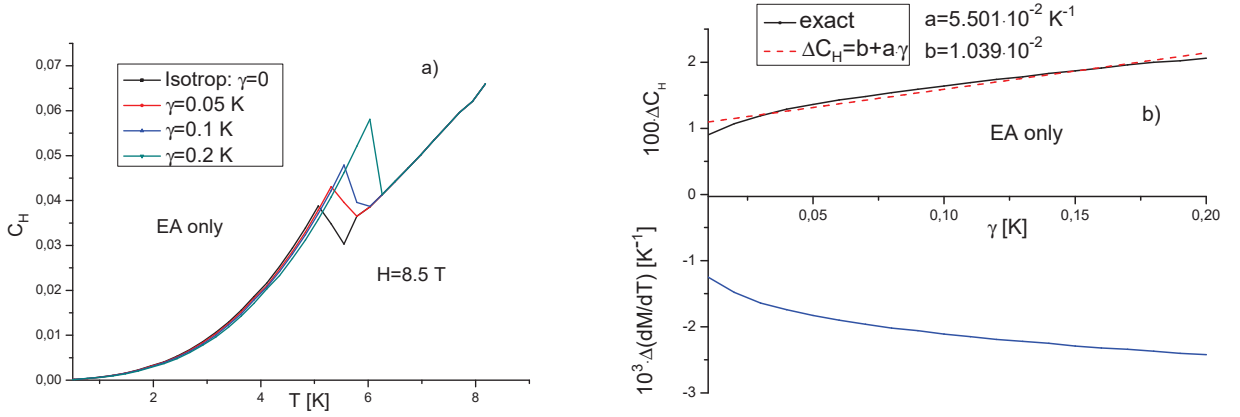


FIG. 5: The heat capacity C_H as a function of temperature with only EA anisotropy (a). Solid lines correspond to the isotropic case with $\gamma = \gamma' = 0$. (b): The discontinuity in C_H (upper panel) and $d\rho/dT$ (lower panel) near $T = T_c$. The dashed curve is a phenomenological fit. The input parameters are the same as in Figs.1. Here one should note that the presence of anisotropies modifies not only C_H but also T_c .

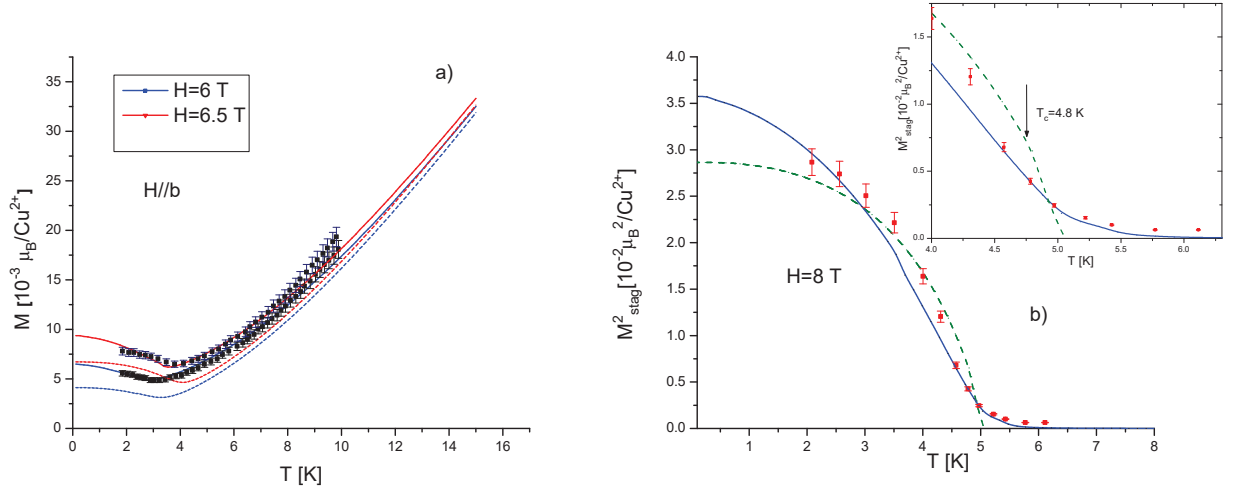


FIG. 6: Uniform (a) and staggered (b) magnetizations for TiCuCl_3 , $H//b$. Solid and dashed lines correspond to the present approximation and approximation in Ref. [28], respectively. Experimental data are taken from Ref. [34]. The optimized parameters are $\gamma = 0.05$ K, $\gamma' = 0.0201$ K and $U = 367$ K. Diamagnetic and other contributions to total experimental magnetizations are taken into account following the ansatz by Dell'amore *et al.* Ref. [40].

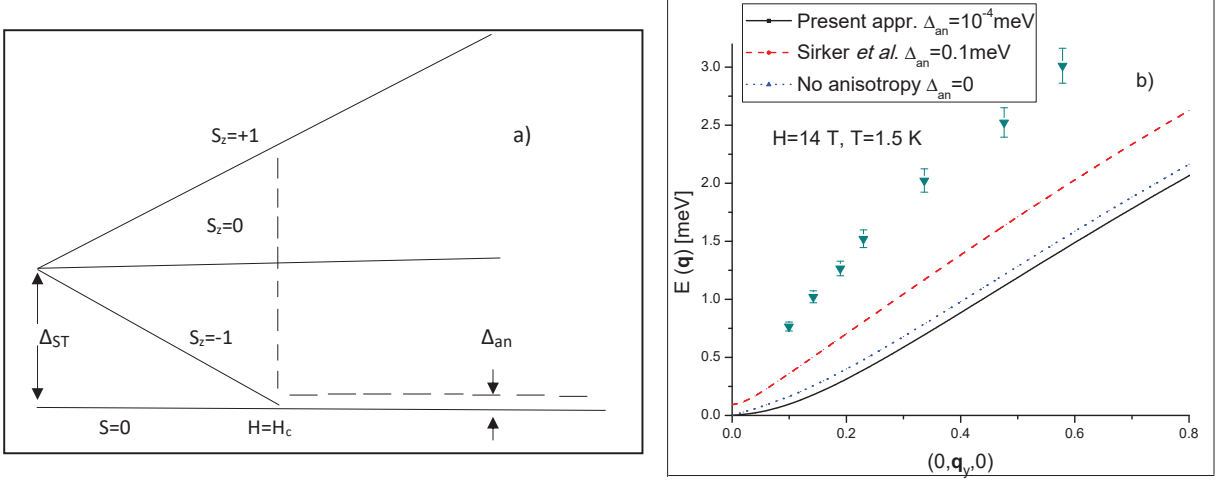


FIG. 7: (a) The schematic illustration of energy levels of a spin-gapped system. At $H = H_c$ the gap Δ_{ST} closes and may reopen due to anisotropies with a tiny gap Δ_{an} . (b) Energy dispersion of the low-lying magnetic excitations in TlCuCl_3 . The solid, dashed, and dotted lines correspond to the present approximation including anisotropies; approximation by Ref. [28] and without anisotropy, respectively. The experimental data are taken from Ref. [44].